Electronic Supplementary Material (ESI) for Journal of Materials Chemistry B.

Supporting information

Development of superior nanotheranostic agents with indocyanine green-conjugated poly(styrene-*alt*-maleic acid) nanoparticles for tumor imaging and phototherapy

Jiale Wang,[a] Chendong Yang,[a] Yanan Gao,[a] and Xuanjun Wu*[,a,b]

[a]National Glycoengineering Research Center, and Shandong Key Laboratory of Carbohydrate Chemistry and Glycobiology, NMPA Key Laboratory for Quality Research and Evaluation of Carbohydrate-based Medicine, Shandong University, Qingdao, Shandong 266237, China

[b]Suzhou Research Institute, Shandong University, Suzhou, Jiangsu 215123, China

Email: xuanjun@sdu.edu.cn

Table of Contents

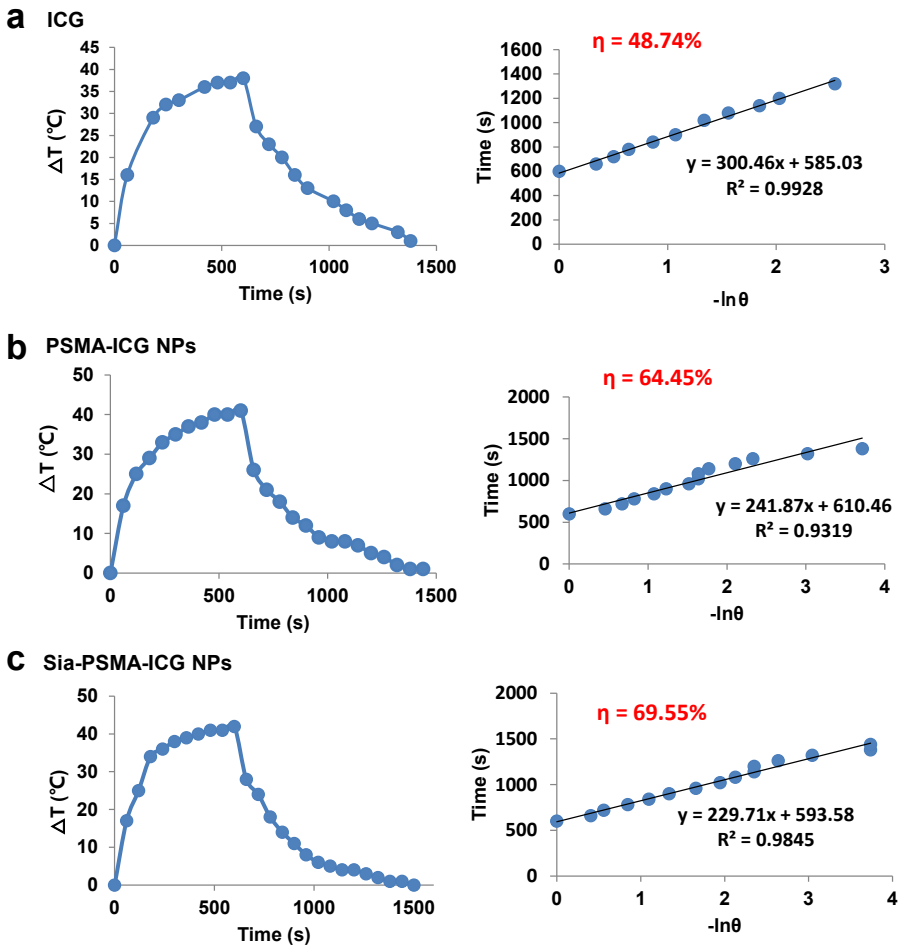

Fig. S1 Photothermal conversion efficiency of ICG, PSMA-ICG NPs and Sia-PSMA-ICG NPs. The photothermal effect and time constant for heat transfer of (a) ICG, (b) PSMA-ICG NPs, and (c) Sia-PSMA-ICG NPs with the same amount of ICG (50 ppm) in PBS (pH 7.4) at 808 nm laser for 600 s and then the light was turned off. It was calculated that the photothermal conversion efficiency of ICG, PSMA-ICG NPs, and Sia-PSMA-ICG NPs was 48.74%, 64.45%, and 69.55%, respectively.

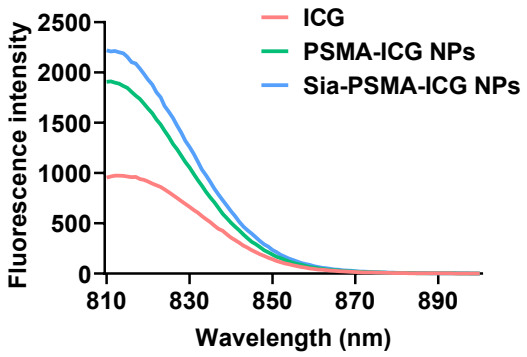

Fig. S2 Fluorescence emission spectrum of ICG, PSMA-ICG NPs, and Sia-PSMA-ICG NPs with the same concentration of ICG (50 ppm) in PBS (pH 7.4).

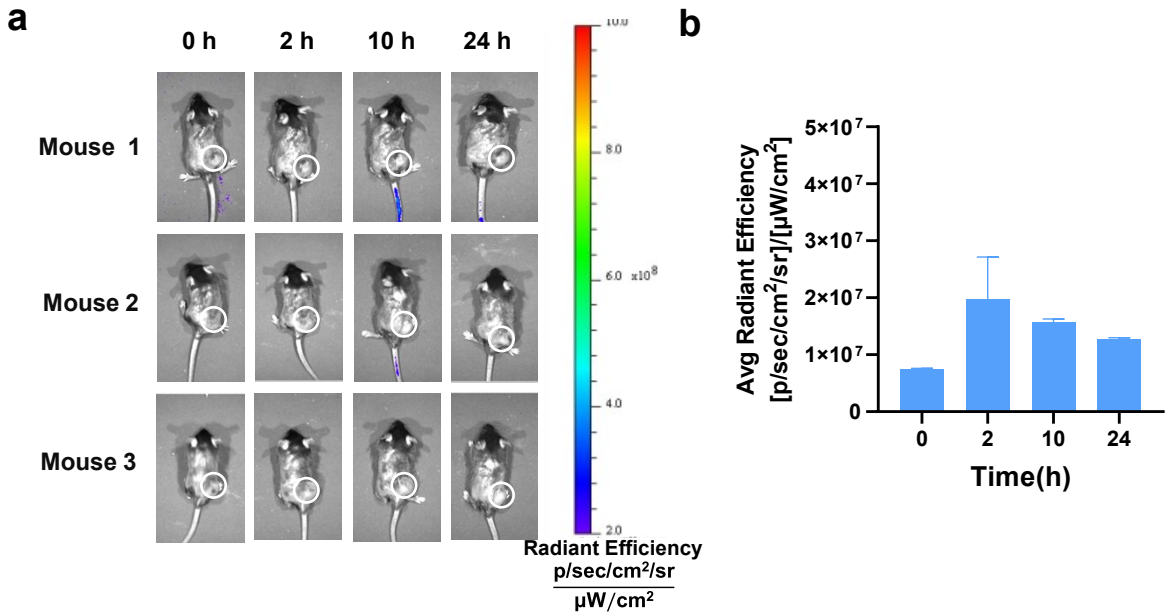

Fig. S3 *In vivo* NIR imaging by PSMA@ICG NPs. (a) *In vivo* fluorescence images of EL4 tumor-bearing mice after injection of PSMA@ICG NPs into these mice through the tail vein with the same amount of ICG (30 µg) per mouse. n = 3 mice per group. (b) Average ICG intensity of tumors in mice over 24 h.

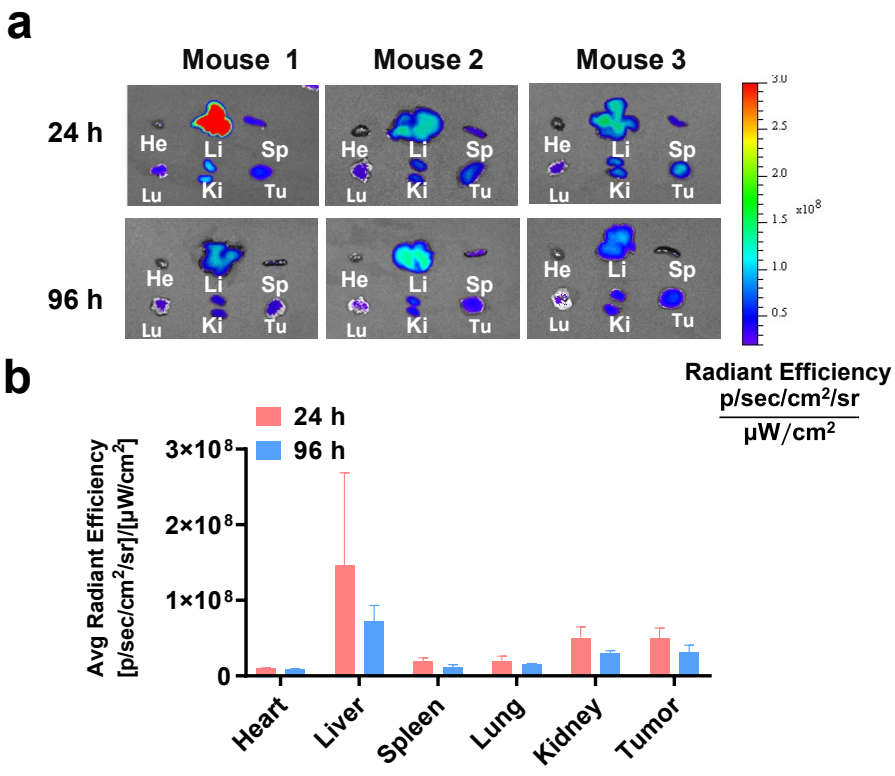

Fig. S4 Biodistribution of PSMA@ICG NPs in EL4 tumor-bearing C57BL/6 mice. (a) Mice-bearing subcutaneous tumors were injected with PSMA@ICG NPs (30 μg of ICG in the NPs) *via* the tail vein. The mice were sacrificed 24 h and 96 h post-injection. *Ex vivo* fluorescence emission of the tumor and representative organs were imaged. $n = 3$ mice for each group.

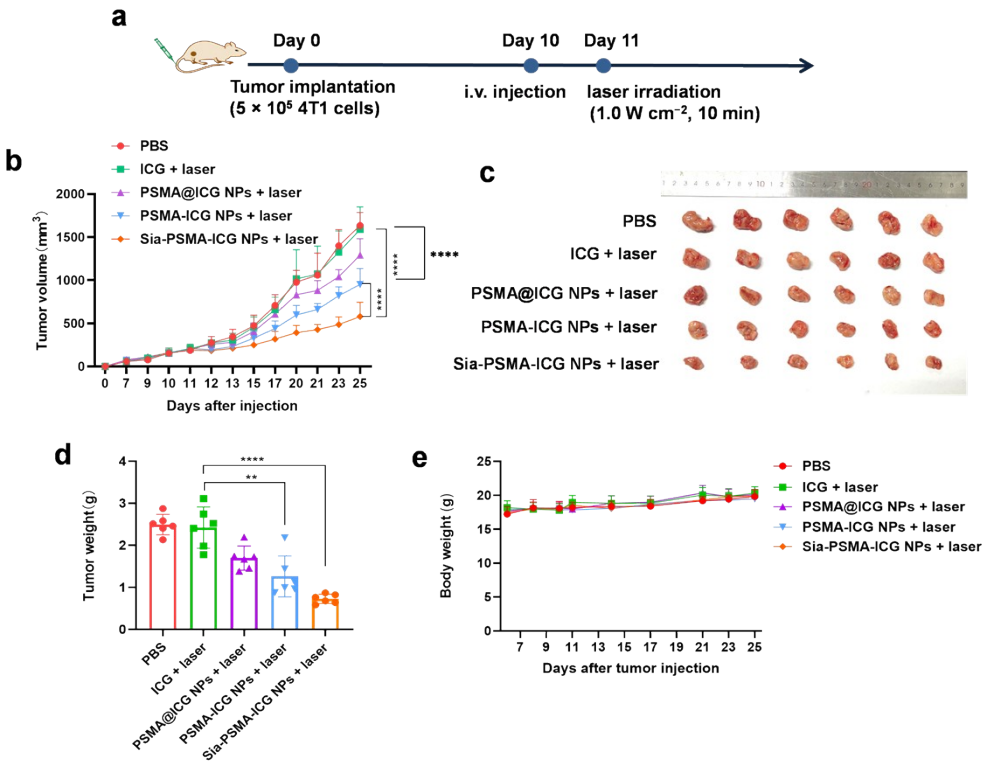

Fig. S5 Photothermal therapy of 4T1 solid tumors. (a) Schematic illustration of the procedure for tumor challenge. (b) Tumor growth curves of mouse groups treated by PBS, ICG + laser, PSMA@ICG NPs + laser, PSMA-ICG NPs + laser, or Sia-PSMA-ICG-NPs + laser. On day 0, 4T1 cells (5×10^5) were injected subcutaneously into BALB/c mice. On day 10, the mice were intravenously injected with PBS, ICG, PSMA@ICG NPs, PSMA-ICG NPs, or Sia-PSMA-ICG-NPs (with the same amount of ICG, 30 μg per mouse) through the tail vein. 24 h later, the tumors were irradiated by the 808 nm laser (1 W cm^{-2}) for 10 min. (c) Photographs of isolated mouse tumors after 25 days. (d) Tumor weight was recorded after the euthanasia of mice on day 25. (e) The body weights of 4T1 tumor-bearing mice. n = 6 mice for each group. GraphPad Prism analyzed the p-value with (b) a two-way ANOVA test or (d) a student t-test. ** $p < 0.01$, **** $p < 0.0001$. The results showed that PSMA-ICG NPs plus laser treatment had a higher antitumor effect than ICG plus laser or PSMA@ICG NPs plus laser treatment, indicating the effectiveness of PSMA-ICG NPs against 4T1 solid tumors. In addition, Sia-PSMA-ICG NPs plus laser therapy showed the best antitumor efficacy in these treatment groups, highlighting the importance of Sia-targeted strategies for treating solid tumors. Notably, antitumor effects can be further enhanced by increasing the dose of injected NPs plus laser.

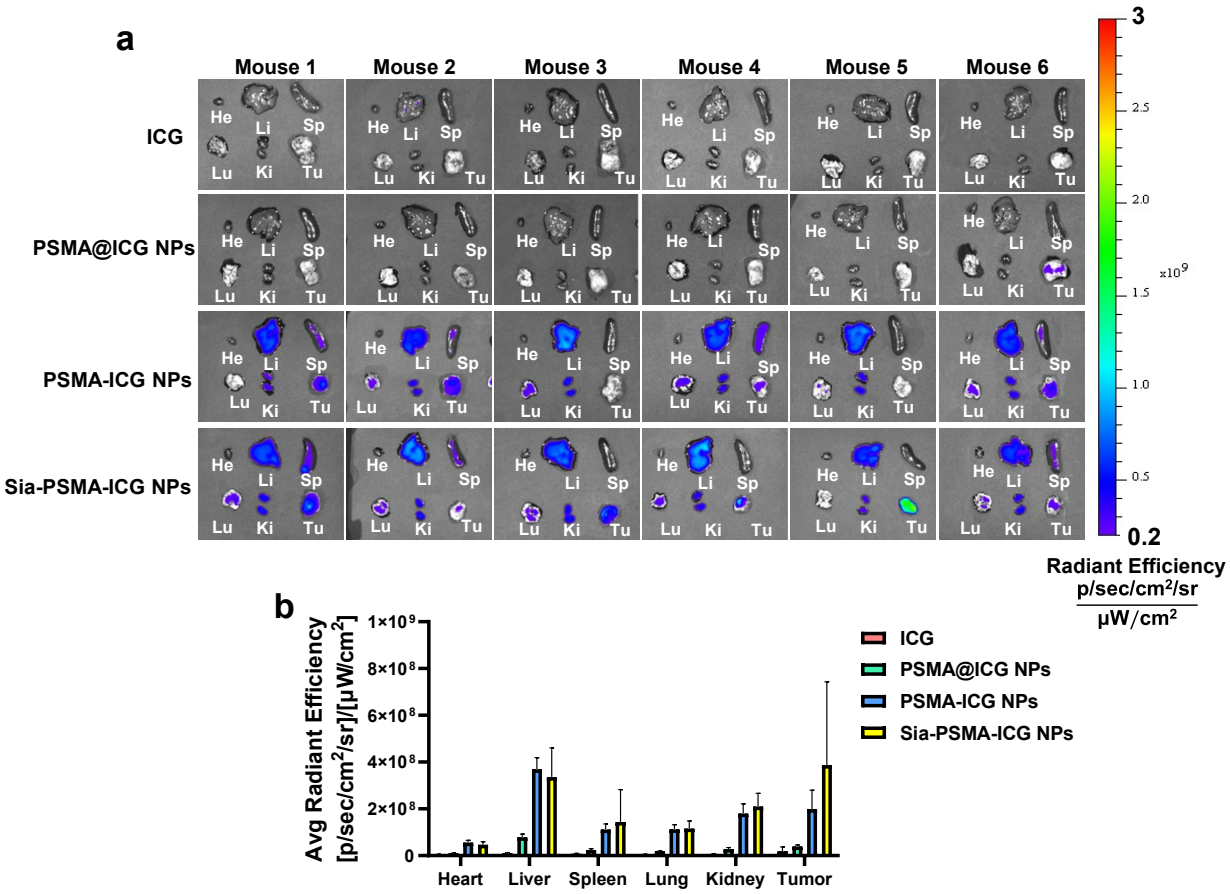

Fig. S6 Biodistribution of ICG, PSMA@ICG NPs, PSMA-ICG NPs, and Sia-PSMA-ICG NPs in tumor-bearing mice after 25 days. To investigate whether PSMA-ICG NPs and Sia-PSMA-ICG NPs were metabolized from the body, the organs and tumors from the mice (see the study in **Fig. S5**) were isolated. *Ex vivo* fluorescence emission of the tumor and representative organs were imaged. Tu, Ki, Lu, Sp, Li, and He represent the tumor, kidneys, lungs, spleen, liver, and heart, respectively. The results showed that after 25 days, the average ICG signal was weak, proving that the NPs can be metabolized from the body.

Materials

Styrene was purchased from Innochem. 2,2'-Azobis (2-methyl propionitrile) (AIBN) were purchased from Aladdin. Maleic anhydride was purchased from Aladdin. ICG-amine (CAS: 1686147-55-6) was purchased from Confluore Biotechnology. Poly(styrene-*alt*-maleic anhydride) (styrene/maleic anhydride = 1:1, MW: 10 kDa, referred to as PSMAn) was obtained from previous studies.[1, 2] Milli-Q (resistivity 18.2 MΩ·cm@25 °C) water was used in the experiments. Other reagents and solvents were purchased commercially and used directly without further purification. EL4 and 4T1 cell lines were cultured in fresh 1640 medium containing 10% fetal bovine serum (FBS), 100 U mL^{-1} penicillin, and 100 μg mL^{-1} streptomycin (2 mM L-glutamine and 1 mM sodium pyruvate) in an incubator containing 5% CO_2. C57BL/6 and BALB/c female mice at 6−10 weeks of age from Shandong University Laboratory Animal Center were used for all studies. The guidelines of the Animal Care and Use Committee of Shandong University conducted all animal experiments.

Preparation of PSMA-ICG NPs and Sia-PSMA-ICG NPs

Preparation of PSMA-ICG NPs. The conjugation of ICG-amine with PSMAn in dimethylformamide (DMF) for 2 h gives the PSMA-ICG polymer. Briefly, to the flask containing 1 mL of DMF was added 10 mg of PSMAn, triethylamine (TEA, 1.6 μL), and ICG-amine (2 mg). After stirring for 2 h at room temperature (RT), the PSMA-ICG polymer was obtained. Then, 1 mL of saturated $NaHCO_3$ was added dropwise to the flask. After stirring for 2 h at RT, the solution was transferred to a dialysis tube (MWCO = 3500 Da). It was dialyzed in water to remove small molecule impurities and solvents. After 2 days of dialysis, the resulting PSMA-ICG NPs were freeze-dried and stored at -20 °C for further studies.

Preparation of Sia-PSMA-ICG NPs. TEA (1.6 μL) and ICG-amine (2 mg) were added to DMF (1 mL) containing 10 mg of PSMAn. After stirring for 2 h at RT, 6.8 mg of 9-amino-Sia[3] was added to the solution. The reaction was performed for 12 h at RT to produce the Sia-PSMA-ICG polymer. Then, the preparation of Sia-PSMA-ICG NPs from the Sia-PSMA-ICG polymer refers to the preparation procedure of PSMA-ICG NPs from the PSMA-ICG polymer.

Synthesis of PSMA@ICG NPs

PSMA@ICG NPs via non-covalent encapsulation of ICG in the PSMA NPs were fabricated by solvent evaporation.[4] Briefly, the chloroform containing ICG (260 μM) was added to the hydrolyzed PSMA solution (2 mg mL^{-1}). Chloroform was then removed by evaporation. The unwrapped ICG was removed by dialysis in water for 2 days. The resulting PSMA@ICG NPs were lyophilized.

Quantification of ICG and 9-amino-Sia

The amount of ICG on the NPs was determined based on ICG absorbance measurements at 780 nm. ICG was determined to be 110 μg and 130 μg/per mg NPs for PSMA-ICG NPs and Sia-PSMA-ICG NPs, respectively. Quantification of 9-amino-Sia on NPs by a colorimetric resorcinol-hydrochloric acid method.[5] The amount of Sia was determined to be 168 μg/per mg NPs for Sia-PSMA-ICG NPs.

Stability of PSMA@ICG NPs, PSMA-ICG NPs, and Sia-PSMA-ICG NPs

ICG, PSMA@ICG NPs, PSMA-ICG NPs, and Sia-PSMA-ICG NPs (20 ppm of ICG) were stored in PBS (pH 7.4) for 0−8 days and their UV-vis NIR absorption spectra were collected daily.

***In vitro* photothermal performance**

ICG, PSMA-ICG NPs, and Sia-PSMA-ICG NPs (0−25 ppm ICG) were added to PBS (pH 7.4), respectively. The solution was irradiated with a near-infrared laser (808 nm, 1 W cm^{-2}) for 10 min. The temperature of the solution is measured every minute. In order to verify their photostability, ICG, PSMA-ICG NPs, and Sia-PSMA-ICG NPs (50 ppm ICG) were added to PBS (pH 7.4). Then, the solution is subjected to five lasers on/off cycles under 808 nm laser irradiation.

Fluorescence properties of PSMA-ICG NPs and Sia-PSMA-ICG NPs

ICG, PSMA-ICG NPs, and Sia-PSMA-ICG NPs (20 ppm ICG) were added to PBS to collect fluorescence spectra with wavelengths from 810 nm to 900 nm.

RBC hemolysis assay

After centrifugation (1000 rpm, 15 min) of the blood collected from mouse legs, the red blood cells (RBCs) were obtained. The RBCs were washed three times with saline until the supernatant was no longer red. The RBCs were then diluted with PBS (0.1 M, pH = 5.5 or 7.4) to 1×10^8 cells per milliliter. The resulting RBCs were incubated in an Eppendorf tube with ICG, PSMA-ICG NPs, or Sia-PSMA-ICG NPs for 1 h at 37 °C (Note that the RBCs were also incubated with PBS as a negative control; the RBCs were incubated with erythrocyte lysate as a positive control). After centrifugation, the supernatant was collected into a new 96-well plate. The absorbance was measured at 541 nm. The calculation formula of hemolysis (%) is as follows:

$$\text{Hemolysis (\%)} = \frac{Abs\ sample - Abs\ 0\%}{Abs\ 100\% - Abs\ 0\%} \times 100$$

Where *Abs* sample, *Abs* 0% and *Abs* 100% represent the absorbance of the sample, the negative control group, and the positive group, respectively.

Photothermal killing of cancer cells by PSMA-ICG NPs and Sia-PSMA-ICG NPs

EL4 cells (1×10^4) were cultured overnight. To the cells were added ICG, PSMA-ICG NPs, or Sia-PSMA-ICG NPs (2 μg, 4 μg, and 8 μg of ICG, respectively). The cells of the laser-treated group are irradiated with a laser (808 nm, 1 W cm^{-2}) for 10 min before incubating for another 10 h. The control group was not subjected to laser irradiation. MTT (3-(4,5-dimethylthiazol-2-yl)-2,5-diphenyltetrazolium bromide) solution was added to each well for 4 h. The cell culture medium was then aspirated, and DMSO was added to the wells (100 μL of DMSO per well). The absorbance at 570 nm was determined. Cell viability is calculated according to the following formula:

$$\text{Cell viability (\%)} = \frac{As - Ab}{Ac - Ab} \times 100$$

Where As, Ab and Ac represent the absorbance values of the wells treated with samples, the blank wells, and the control wells treated with PBS, respectively.

In vivo NIR imaging and biodistribution

5×10^5 EL4 cells were injected into each mouse. After 8 days, the solution of ICG, PSMA-ICG NPs, or Sia-PSMA-ICG NPs (containing 30 μg ICG) in PBS (100 μl) was injected into tumor-bearing mice via the tail vein. Then, *in vivo* NIR fluorescence imaging was performed at 0−168 h after injection of ICG or the NPs, respectively. At 24 h after injection, the mice were sacrificed by anesthesia. Their tumors and representative organs were dissected and analyzed for *ex vivo* fluorescence imaging (n = 3 mice per group).

Photothermal therapy of tumors

For EL4 tumor challenge study, C57BL/6 mice were injected subcutaneously with EL4 cells (5×10^5) on day 0. When the tumor grows to an average of 300 mm^3 (on day 8), PBS, ICG, PSMA-ICG NPs, or Sia-PSMA-ICG NPs were injected intravenously into EL4 tumor-bearing mice (n = 6 mice per group). The mice were irradiated with the 808 nm laser (1.0 W cm^{-2}, 10 min) at 12 h following injection of ICG or the NPs in mice. (Note: It can be seen from **Fig. 7a** in the main text that the tumor signal is most potent when injected into NPs for 168 h, but the tumor is too large. Therefore, photothermal therapy is performed at a shorter time-point (12 h) following the injection of ICG or the NPs in mice.) For 4T1 tumor challenge study, BALB/c mice were injected subcutaneously with 4T1 cells (5×10^5) on day 0. On day 10, PBS, ICG, PSMA@ICG NPs, PSMA-ICG NPs, or Sia-PSMA-ICG NPs were injected intravenously into 4T1 tumor-bearing mice (n = 6 mice per group). The mice were irradiated with the 808 nm laser (1.0 W cm^{-2}, 10 min) at 24 h following injection of ICG or the NPs in mice. Tumor volume and mouse body weight are measured daily. Tumor volumes are calculated with the formula: Volume (mm^3) = 1/2 (length × width × height)[6].

References

1. X. Wu, Y. Tian, M. Yu, J. Han and S. Han, *Biomater. Sci.*, 2014, **2**, 972–979.
2. Z. Li, Y. Song, Y. Yang, L. Yang, X. Huang, J. Han and S. Han, *Chem. Sci.*, 2012, **3**, 2941–2948.

3. B. Lin, X. Wu, H. Zhao, Y. Tian, J. Han, J. Liu and S. Han, *Chem. Sci.*, 2016, **7**, 3737–3741.
4. V. B. Rodriguez, S. M. Henry, A. S. Hoffman, P. S. Stayton, X. Li and S. H. Pun, *J Biomed Opt*, 2008, **13**, 014025.
5. L. Svennerholm, *Biochim. Biophys. Acta*, 1957, **24**, 604–611.
6. M. M. Tomayko and C. P. Reynolds, *Cancer Chemother. Pharmacol.*, 1989, **24**, 148–154.